Aggregated initiators: defining their role in the ROP of rac-lactide

Journal Name

ARTICLE

Aggregated initiators: Defining their role in the ROP of *rac*-lactide

Jean-Marie E. P. Cols,[a] Victoria G. Hill,[a] Stella K. Williams[a] and Ruaraidh D. McIntosh*[a]

Received 00th January 20xx,
Accepted 00th January 20xx

DOI: 10.1039/x0xx00000x

www.rsc.org/

Reported examples of aggregated initiators for the ring-opening polymerisation (ROP) of lactide often lack detailed investigations as to the nature of the active species, making it difficult to reconcile ligand design with performance. Here, we offer additional stability to the polynuclear titanium complexes, Ti**L**(O*i*Pr) (**L** = **9**-**14**), through a bridging carboxylate anchored to the supporting amine bis(phenolate) ligands. An in-depth study of solution-state behaviour determined the process of assembly was driven by interactions between the carboxylate and a vacant site on a neighbouring titanium centre. Furthermore, we establish that mononuclear units form dynamic mixtures of polynuclear aggregates, with a clear relationship between nuclearity of the aggregates and the steric bulk on the ligand. Smaller aggregates displayed increased activity towards the ROP of *rac*-lactide. Furthermore, addition of a chiral centre, on the ligand framework, was investigated as a route to influence the selectivity of the polymerisation via an easily-accessible initiators.

Introduction

Single-site, Lewis acidic metal centres are often applied to the ring-opening polymerisation (ROP) of lactide as these are well defined initiators that provide high levels of control over the polymerisation process. While these initiators show high activity towards the ROP of lactide,[1] some can lack stability outside of the glovebox. Polynuclear or aggregated initiators generally have improved stability[2] but structure-activity relationships are more challenging to establish for these species due to complications associated with defining their nuclearity in solution.[3-10]

Aluminium isopropoxide is a well-studied example of an aggregate that applied to the ROP of lactide.[11,12] It was reported that trinuclear and tetranuclear aluminium clusters, bridged by the isopropoxide ligand, were formed under the polymerisation conditions. The trinuclear species was found to be the more reactive and more abundant of the two species. Furthermore, varying the conditions of the reaction to promote formation of the trinuclear species resulted in a decrease in the PDI of the polymer. This increase in control was attributed to the exchange between the trinuclear and tetranuclear species which disrupts propagation.

Further examples of metal alkoxide aggregates include a group of compounds with general formula $M_5(\mu_5\text{-}O)(OR)_{13}$ (M = Fe, Y, La, Sm, Yb; *R* = alkyl). In the case of M = Y,[13] similar levels of activity in the ROP of lactide was reported for the pentanuclear and mononuclear activators, suggesting that larger aggregates can retain the activity of the monometallic complexes. In the work of Tolman et al. (M = Fe),[14] the activity of the pentanuclear activator was found to be similar to a dinuclear activator but in contrast, a different iron(III) system, found the dinuclear species to be more active than the mononuclear species.[15] These studies highlight that the relationship between aggregate size and activity is not straightforward.

The aforementioned examples are polynuclear complexes[13-15] bridged by alkoxide ligands. These ligands are labile by definition, as they also act as initiating groups in the ROP of lactide and therefore have limited control over cluster stability. Here, a multidentate amine bis(phenolate) ligand is bound to the metal during the polymerisation process. Utilising an amino acid,[16] we can incorporate a pendant carboxylate arm into the ligand, which is capable of providing a stabilising, bridging interaction between two metal centres and promote stability of the aggregates. The polynuclear complexes presented herein represent out first efforts in the synthesis of polynuclear titanium initiators for the ROP of *rac*-lactide that are assembled and stabilised through ligand design.

Results and Discussion

Ligand synthesis and characterisation

Starting from the amino acid glycine, two synthetic routes were used to access compounds **1**-**4**$(H)_3$: two successive reductive aminations were required to obtain compound **1**$(H)_3$ while a one-pot Mannich condensation reaction produced compounds **2**-**4**$(H)_3$.[17-19] Altering the peripheral substituents on the phenol rings allowed for analysis of structural trends in assembling a polynuclear titanium complex as well as assessing the tunability of the polynuclear titanium initiators for the ROP of lactide. Varying the starting amino acid, from glycine to alanine or phenylalanine, allows the incorporation of a chiral centre onto the pendant arm of the ligand. This allows us to assess the effect

Institute of Chemical Sciences, Heriot-Watt University, Riccarton, Edinburgh, EH14 4AS, UK. E-mail: R.McIntosh@hw.ac.uk.

Electronic supplementary information (ESI) available. CCDC 1562058 and 1562059.

For ESI and crystallographic data in CIF or other electronic format see. See DOI: 10.1039/x0xx00000x

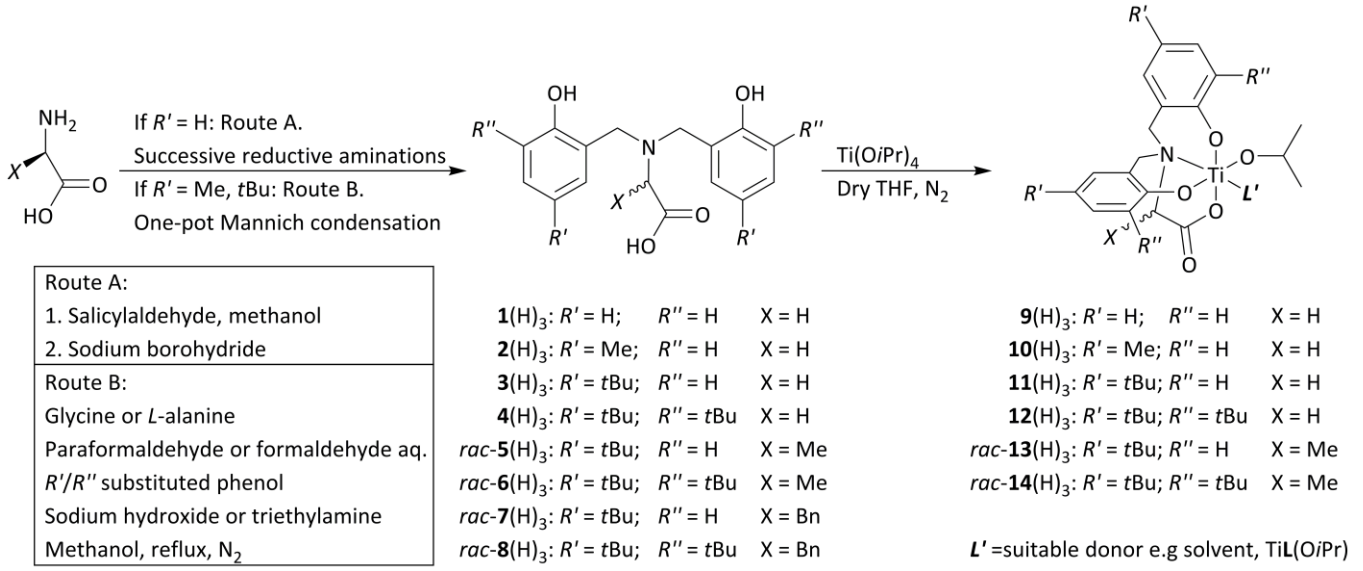

Scheme 1. Summary of synthetic routes to ligand precursors 1-8$(H)_3$ and proposed mononuclear forms of titanium isopropoxide complexes **9**-**14**, where *L′* denotes a suitable donor moiety.

it has on aggregation as well as its ability to influence the stereoselectivity of the polymerisation. A reported procedure for the synthesis of enantiomerically pure *S*-**6**$(H)_3$ was initially followed[20] but several attempts to obtain the optically pure compound were unsuccessful as polarimetry indicated the compound had racemised under the relatively harsh conditions of the reaction.[21-23]

We sought to synthesise compounds **5**-**8**$(H)_3$ in higher yields using the reaction conditions previously employed in the synthesis of compounds **2**-**4**$(H)_3$.[17-19] Unreacted phenol was removed by acidifying the reaction mixture in methanol with 1 M aqueous hydrochloric acid and collecting the resulting solids. Further purification by column chromatography gave the pro-ligands in high purity. Despite attempts to optimise the methodology, the isolated yields for **7**$(H)_3$ and **8**$(H)_3$ were unsatisfactory (< 5 % yield). We interpreted the cause as the bulkier benzyl group in the *X* position of **7**$(H)_3$ and **8**$(H)_3$, which would sterically hinder the attack of the phenol on the imine/iminium ion during the electrophilic aromatic substitution step in the mechanism of the Mannich condensation, especially during the addition of the second phenol group. Indeed the monophenolate analogue of **8**$(H)_3$ was isolated from the reaction (see Supporting Information). Heating to reflux in higher boiling solvents was attempted to increase yields but this was ultimately unsuccessful in producing sufficient quantities of **7**$(H)_3$ or **8**$(H)_3$ for further reaction.

Characterisation of **1**-**6**$(H)_3$, by ^1H and ^{13}C NMR spectroscopy, showed the expected products had been obtained. However, in the cases of **5**$(H)_3$ and **6**$(H)_3$, the spectra were more complex than had been expected. Bond rotations about the methylene bridges result in magnetically inequivalent environments due to the magnetic anisotropy of the phenol rings and the presence of the chiral *X* group. This was verified by EXSY NMR experiments that confirmed these signals were under exchange. In addition, the methylene protons for **5**-**6**$(H)_3$ are no longer observed as singlets, appearing as separate doublets for each diastereotopic protons.

Large, colourless, block crystals of **6**$(H)_3$ were grown from a saturated methanol solution. These were analysed by SCXRD using Cu radiation to determine the absolute configuration of the molecule by anomalous dispersion. The molecule was determined to be in the *S*-configuration with high certainty shown by the reported flack parameter of 0.00(2). Unfortunately this single crystal sample was found to not be representative of the bulk sample.

Polarimetry was used to examine the enantiopurity of **5**$(H)_3$ and **6**$(H)_3$. In both cases it was found that, in the bulk samples, the *S*-amino acids had racemised during the Mannich condensation reaction to give *rac*-**5**$(H)_3$ and *rac*-**6**$(H)_3$.

Dynamic polynuclear titanium complexes.

A ligand substitution reaction was employed to synthesise titanium complexes **9**-**14** using titanium isopropoxide as the source of titanium. Compounds **1**-**6**$(H)_3$ were stirred in dry THF under a dry N_2 atmosphere. Following the addition of titanium isopropoxide, an instant change from cloudy white suspension to a clear yellow/orange solution occurred. The exception was compound **1**$(H)_3$ which, when treated with titanium isopropoxide, swiftly formed a yellow precipitate.

Following the examples of other amine bis(phenolate) complexes from the literature,[24-26] the complexes in Scheme 1 were proposed to form in the first instance. Considering the preference of amine bis(phenolate) titanium complexes for a six-coordinate geometry, this would leave one coordination site on the titanium centre occupied by a labile donor, ***L′*** *(e.g.* solvent*)*.

The aforementioned yellow precipitate from the reaction of compound **1**$(H)_3$ and titanium isopropoxide was identified as compound **9** by mass spectrometry. Solution-based characterisation was not possible since compound **9** was largely

insoluble in common laboratory solvents. However, CPMAS NMR was used to obtain data that supported characterisation by mass spectrometry and elemental analysis.

The NMR spectra of **9**-**14** in $CDCl_3$ were more complex than anticipated. By integrating the broad regions in these spectra, the expected integrals for the aromatic, methylene, *R*'/*R*'' and isopropoxide groups are present, indicating that the compounds were formed. EXSY experiments revealed an exchange process was the effect behind the larger number of peaks in these complex spectra. We attributed the nature of **10**-**14** in solution to the dynamic coordination of a variety of labile donors present in solution. As a representative example, the ^{1}H NMR spectrum of **12** was repeated in dry D6-DMSO, a strong donor solvent that could inhibit exchange and/or aggregation. Indeed, we observed significantly fewer signals in a far less complex spectrum in comparison to the spectrum of **12** in $CDCl_3$. However, multiple species under exchange were still present. This confirmed that a strong donor could slow the exchange process and supported our proposition that the vacant site was integral to the exchange process. Further to this, 4-dimethylaminopyridine (DMAP) was added to an equimolar quantity of the complexes in $CDCl_3$. The ^{1}H NMR spectra of the samples showed the presence of a single species in solution with DMAP under exchange. These detailed experiments confirm the proposed structures of **9**-**14** exist in solution and that the nature of the species is solvent dependent. A feature in all of the ^{1}H NMR spectra of **9**-**14** with DMAP in $CDCl_3$ is the significant line broadening of the methylene bridge protons. We interpret this as an indication that the ligand framework is flexible despite coordination to Ti. Through-space contacts between protons on the pendant carboxylate, phenolate moieties in the ligand framework, and DMAP are clearly defined in the well-resolved spectra of **12** and *rac*-**14**. This evidence placed a DMAP binding at the ***L'*** position.

Crystals of **12** were grown from a saturated, dry THF solution and analysed by SCXRD. The structure obtained showed a trinuclear form of **12** had been crystallised, whereby the three Ti atoms are linked by carboxylates and one terminal Ti is coordinated to propan-2-ol (Figure 1). This terminal propan-2-ol can be distinguished from the isopropoxides in the structure with its longer O–Ti bond length (2.091(2) Å versus 1.771(2) Å) as well as the freely-refined proton that was located in the difference Fourier map (attached to O16). The D···A and H···A distances of 2.556(3) Å and 1.80(4) Å respectively are within expected hydrogen bonding values.[27] The longer O–Ti bond length of 2.091(2) Å was found to be in agreement with other neutral propan-2-ol titanium complexes (Figure S2). Furthermore, no counter-ions are present in the asymmetric unit. Analysis of the average native and bridging carboxylate O–Ti (2.058(2) and 2.063(2) Å) and C–O (1.261(3) and 1.255(3) Å) bond distances are in agreement with related structures.[19,28,29] The similarity in bond distances between native and bridging interactions supports the view that the carboxylates are delocalised in their bridging interaction with the titanium centres in the structure.

Crystals of **12**$_3$(HO*i*Pr) were dissolved in $CDCl_3$ and a ^{1}H NMR spectrum obtained. Comparing this spectrum with that of the original dynamic mixture of **12** revealed that the trinuclear form obtained in the solid state crystal structure forms part of the mixture. After leaving the dissolved crystals of **12**$_3$(HO*i*Pr) in $CDCl_3$ for one day at RT under a dry N_2 atmosphere, further ^{1}H NMR spectra were taken to reveal the trinuclear aggregate had reverted to the dynamic mixture previously observed. This was strong evidence that the mixtures observed by ^{1}H NMR spectroscopy of **10**-**14** are of a pure product undergoing dynamic exchange in solution, where each spectrum displays an equilibrium of species of differing nuclearity in solution. In both the ^{1}H NMR spectra of **12**$_3$(HO*i*Pr) and **12**, a sharp doublet is noticeable at 10.41 ppm. A key feature in the crystal structure is the intramolecular hydrogen bond between the propan-2-ol bound to Ti1 and a carboxylate native to Ti3. The ^{1}H COSY NMR experiment showed this proton is coupling with a proton at 4.36 ppm, which corresponds to the expected chemical shift of an propan-2-ol C*H*. This coupling would explain why this appears as a doublet with a typical vicinal coupling constant of 7.60 Hz. An EXSY NMR experiment shows an exchange signal that corresponds to the propan-2-ol O*H* at 1.60 ppm. From this evidence, we propose this doublet to arise from the intramolecular hydrogen bonded propan-2-ol O*H*. The presence of the doublet at 10.41 ppm in both the spectra of the crystals of **12** and the dynamic mixture of **12** confirms the solid-state trinuclear structure exists in solution as part of the dynamic mixture. Further analysis by ^{1}H COSY and ROESY NMR experiments both concur with the proposed dynamic nature of **10**-**14**, whereby through-bond and through-space coupling was present for the varied species in solution. By focusing on specific regions of these spectra, we could tentatively estimate the nuclearity of the aggregates in the dynamic mixture. For example, we noted that the ^{1}H NMR spectrum of **11** in $CDCl_3$ was better resolved with a set of signals with similar intensity in the methylene region. A COSY experiment showed there were nine pairs of diastereotopic protons, which correspond to a trinuclear aggregate.

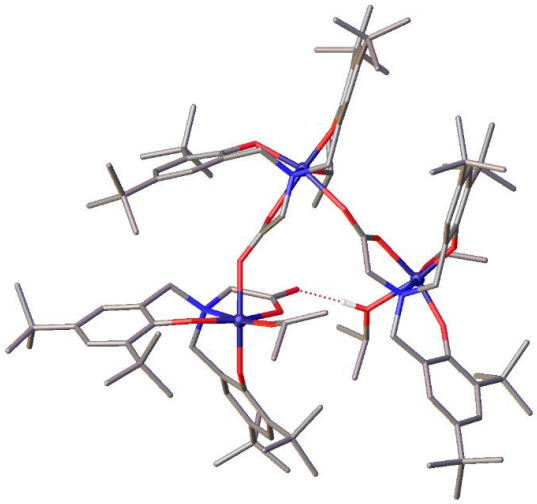

Figure 1. Crystal structure of **12**$_3$(HO*i*Pr) with formula [Ti**4**(O*i*Pr)]$_2$[Ti**4**(O*i*Pr)(HO*i*Pr)]. Ligand framework displayed as tubes. Hydrogen atoms omitted for clarity with exception of the proton that displays an intramolecular hydrogen bond (dashed red lines) between the isopropanol ligand and the carboxylate native to Ti1. Ti = purple; C = grey; N = blue; O = red, H = white.

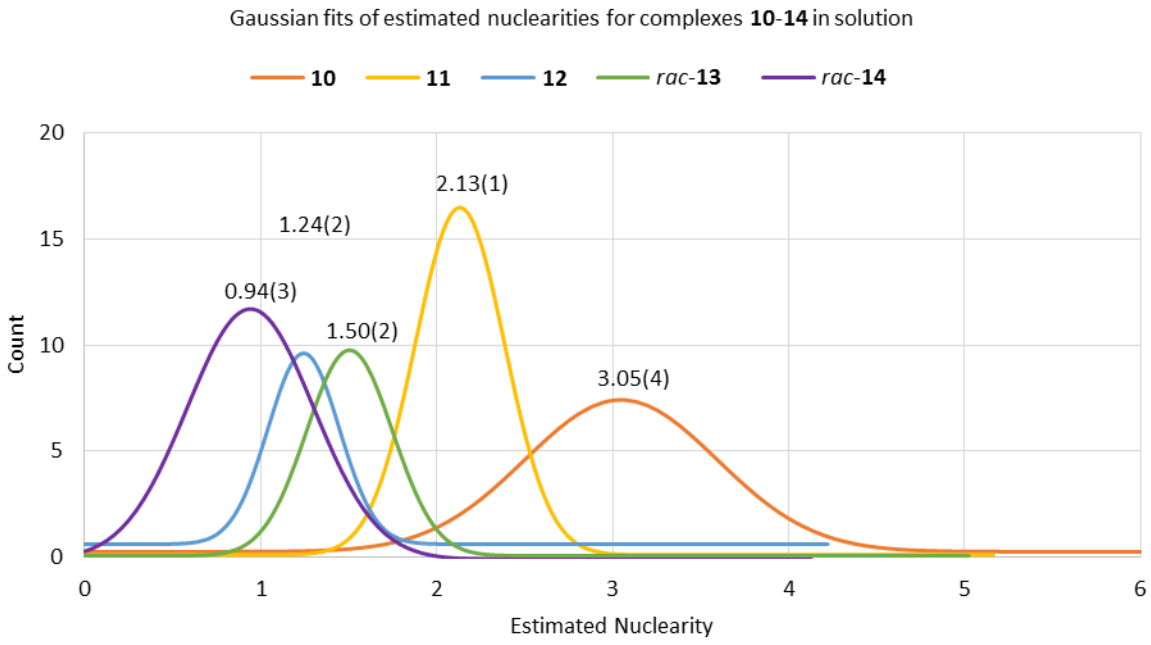

Figure 2. Plot of Gaussian fitting curves for datasets of estimated nuclearities of **10**-**14** in $CDCl_3$ versus the count of data points corresponding to said nuclearity. The estimated nuclearities were obtained by ^{1}H DOSY NMR experiments via estimated *MW*s. See Supporting Information for further details.

Using ^{1}H COSY and ROESY NMR experiments, we tentatively found the possibility of trinuclear/tetranuclear aggregates under exchange for **10**, dinuclear/trinuclear aggregates for **12** and mononuclear/dinuclear aggregates for **13** and **14**. A more detailed analysis is provided in the Supporting Information.

Having observed aggregation in the crystal structure of **12**, we sought to gain insight into the extent of aggregation in samples of **10**-**14** in solution. A ^{1}H DOSY NMR experiment would allow the determination of the diffusion coefficients of the species in solution that can be used to estimate the MWs of the aggregates using external calibration curves (ECCs). These ECCs, published by Stalke and coworkers,[30,31] take into account variables when measuring the diffusion coefficient such as the solvent, analyte shape and concentration, temperature and the spectrometer used. The authors noted that the ECCs worked well for a particular molar density range. Molecules with heavy atoms, in relation to organic atoms, exceed the molar density range stated for the ECCs, which results in an underestimation of the *MW*. For the analytes studied here, the heavier titanium atom leads us to expect an underestimation of *MW* that will be consistent throughout **10**-**14**. For further details, refer to the Supporting Information.

Estimated *MW* distributions were obtained for compounds **10**-**14** using the most appropriate ECCs. A Gaussian distribution was fitted for each dataset to estimate the mean size of the distributions. Figure 2 overlays the *MW* distributions of compounds **10**-**14**. As expected, an increase in the steric bulk at the *R*′/*R*′′ positions of **10**-**12** results in a decrease in the size of the aggregates in solution. The same effect was associated when adding the *X* group in *rac*-**13** and *rac*-**14**. The dynamic nature of the aggregates in solution and the overlapping of signals in the NMR spectra can result in an average diffusion coefficient being estimated from a signal, resulting in broadening of the distributions presented here. The estimated nuclearities of the compounds correlate with the observations made previously by EXSY, COSY and ROESY NMR experiments. Using the aggregated structure **12**$_3$(HO*i*Pr), we can look at how bulk in the *R*′/*R*′′ positions affect aggregation. Close steric interactions between C24D/C47C show how bulk in the *R*′′ position impedes aggregation. Importantly, close proximity between C12/C29B and C22/C45C demonstrates how bulk in the *R*′ also hinders aggregation, explaining the trends observed for the aggregation of compounds **10**-**12**.

The proposed structures (Scheme 1) are based on the evidence from the crystal structure of **12** as aggregates of the mononuclear form of **12**, which is composed of a single titanium centre bound by ligand **4** and an isopropoxide. It should be noted that the dynamic nature of this system limits our ability to probe the structures present in the mixture. Further conceivable entities in solution are aggregates with various donors at the vacant site (bridging carboxylate, propan-2-ol, isopropoxide). The ambidentate nature of the carboxylate arm allows ligands **1**-**6** to switch from LX_3 to L_2X_2 type donation, allowing for both L- and X-type donors on the vacant site.

In comparison to **10**-**14**, complex **9** was not able to be studied to the same level of detail due to its heterogeneity. This highlights the challenges faced in understanding a heterogeneous system in comparison to a homogeneous analogue.

Application in the ROP of *rac*-lactide

The low relative cost and toxicity of Ti(IV) make it a highly desirable initiator for the production of a biodegradable

polymer with applications where leaching of a toxic metal is of great concern.[32-34]

The performance of complexes **9**-**14** was studied in the ROP of *rac*-lactide to investigate how the ligand design and nuclearity of the complexes affect the polymerisation process. We found ambiguity relating the nuclearity of polynuclear species to their performance in the ROP of lactide. The in-depth understanding of the solution-state behaviour of polynuclear will be key in allowing us to draw conclusions between performance and structure. Furthermore, our aim was to determine the extent of stereocontrol that could be imparted by the chiral *X* group in *rac*-**13** and *rac*-**14** despite the high temperature (130 °C) and dynamic nature of the complexes. The data collected from these experiments is summarised in Table 1. The monomer-to-titanium loadings were calculated assuming the solid samples were of the pure mononuclear forms of **10**-**14**.

Compound **9** showed near-zero conversions under various polymerisation conditions and thus no polymer characterisation data could be gathered. This can be explained by the heterogeneous nature of the compound hampering access to the active sites on the titanium centre. Using the more soluble analogues of **9** with alkyl *R*′/*R*′′ groups was key to achieving an active compound for the ROP of *rac*-lactide.

By comparing the conversion achieved by **10**-**12** under different $[M]_0/[Ti]_0$ loadings under solution polymerisation conditions, an increase in activity described by **10** < **11** < **12** was apparent. The significant difference in performance was unexpected for a simple change from methyl to *tert*-butyl to di-*tert*-butyl *R*′/*R*′′ groups, prompting us to further investigate the underlying cause.

Having observed aggregation to be a feature of these complexes, we sought to investigate the tendency of **10**-**12** to aggregate in solution. The ^{1}H DOSY NMR data revealed the complexes formed larger aggregates in the order **10** > **11** > **12**, which correlated with the increase of steric bulk from **10** to **11** to **12**. Since aggregational effects would compete with the monomer and polymer chains for time on the active site on the titanium centre, it would follow that a greater tendency for aggregation would lead to a decrease in activity. For this reason, we propose aggregational effects to correlate with the activity of these compounds, whereby **10** exhibits low activity in solution due to its propensity to aggregate while **12** has a lower tendency to aggregate and displayed better performance than **10** or **11**. In these systems comprised of dynamic polynuclear aggregates, we found reducing nuclearity resulted in increased activity towards the ROP of *rac*-lactide. Other systems[10-14] typically found nuclearity to have little or no effect on performance. In contrast, some systems with metal centres supported by multidentate ligands[15,35] showed the mononuclear form to be the most active form. Our observations agree with these systems whereby the additional unit(s) during aggregation cause an increase in steric bulk around the active site.

Further studies of **10**-**12** under melt polymerisation conditions were undertaken with 300:1 monomer:titanium loading in a sealed flask for 24 h. Under these conditions, all three compounds **10**-**12** achieved high conversion after 24 h. To reveal differences in activity between these compounds, the polymerisation time was reduced. Conversion fell below 15% when the polymerisation time was 2 h and efforts to recover the polymer were unsuccessful, an indication that short chains were synthesised. A polymerisation time of 6 h was successful in revealing the difference in activity between compounds **10**-**12**. The PDI values are consistently lower for **12** in comparison to **10** and **11**. This can be explained by the *tert*-butyl *R*′′ group that imparts greater control over the polymer formed, which is in accord with what is found for a variety of other ROP of lactide systems.[24,36,37] Increasing the extent of alkyl groups through the *R*′/*R*′′ groups on the titanium initiators **10**-**12** correlates with an increase in conversion. In contrast to what was observed under solution polymerisation conditions, compound **11** is more active than compound **12** under melt conditions. The difference between **11** and **12** is the additional *tert*-butyl group in the *R*′′ positions, which primary contribution will be greater steric bulk around the active site on the titanium centre. Under melt polymerisation conditions, *rac*-lactide acts as a strong donor solvent that will reduce the extent of aggregation much like when using strong donors during NMR characterisation of these complexes. We propose that the *tert*-butyl group in the *R*′′ position for initiator **12** would sterically hinder the interaction of the monomer and polylactide chains with the titanium centre, resulting in a reduced activity in comparison to compound **11**. To summarise, aggregation effects are proposed to be less pronounced under melt conditions and are outweighed by the extent to which the monomer and growing chains can access the active site. Further testing of the catalytic system under melt conditions was undertaken by increasing the monomer:titanium ratio to 600:1 for compounds **11** and **12**. A slight decrease in the conversion was observed in comparison to a monomer:titanium ratio of 300:1. In addition, the M_n values are similar, which is unexpected as a lower loading of active sites typically leads to decreased polymer chain lengths. In this case, the values obtained for conversion, M_n and $M_{n(NMR)}$ are similar despite reducing the number of active sites by half. This is indicative of polymeryl exchange, which we attribute to the high temperature (130 °C) of the reaction and competing aggregation of the initiator.

Ligand influence over stereoselectivity

Stereoselective ROP of *rac*-lactide is sought to control the tacticity of the resulting polylactide product. Increasing the isotacticity of polylactide has been shown to influence the properties of the polymer product and altering these is essential for the successful application of polylactide in the plastics industry and widen its potential uses.[38,39]

Compounds **11** and **12** were the most active initiators for the ROP of *rac*-lactide under both solution and melt polymerisation conditions. For this reason, using the analogous compounds *rac*-**13** and *rac*-**14** provide an opportunity to examine the effect of adding a chiral centre to the ligand. For the initiator *S*-**14** we see that there are two potential sites for polymerisation on the Ti centre (Figure 3). In the crystal structure, site ***A*** is bound by the isopropoxide initiating group while site ***A**** is bound by the

Solution polymerisation conditions ([M]$_0$ = 1 mol·L^{-1}, dry toluene, oil bath temperature 130 °C)							
Entry	Activator	[M]$_0$/[Ti]$_0$	Time	Conv.[a]	M_n[b]	$M_{n(NMR)}$[c]	PDI[d]
1	**10**	20	24 h	4	-		-
2	**10**	100	24 h	0	-		-
3	**11**	20	24 h	92	4120	7260	1.24
4	**11**	50	24 h	13	-		-
5	**11**	100	24 h	19	4070	4790	1.09
6	**12**	50	24 h	90	7360	11300	1.24
7	**12**	100	24 h	62	9420	13500	1.18
8	*rac*-**13**	20	24 h	86	6080	4780	1.54
9	*rac*-**13**	50	24 h	26	4400	4330	1.24
10	*rac*-**13**	100	24 h	13	-	-	-
11	*rac*-**14**	20	24 h	93	4050	5640	1.27
12	*rac*-**14**	50	24 h	59	5260	5880	1.22
Melt polymerisation conditions (oil bath temperature 130 °C)							
Entry	Activator	[M]$_0$/[Ti]$_0$	Time	Conv.[a]	M_n[b]	$M_{n(NMR)}$[c]	PDI[d]
13	**10**	300	2 h	5	-	-	-
14	**10**	300	6 h	21	5040	4640	1.32
15	**10**	300	24 h	83	10000	9810	1.47
16	**11**	300	2 h	18	-	-	-
17	**11**	300	6 h	74	13500	13000	1.64
18	**11**	300	24 h	96	15000	10700	1.54
19	**11**	600	24 h	93	14800	11800	2.03
20	**12**	300	2 h	14	-	-	-
21	**12**	300	6 h	47	6780	8320	1.26
22	**12**	300	24 h	89	14100	12000	1.40
23	**12**	600	24 h	80	12200	11500	1.39
24	*rac*-**13**	300	2 h	45	6300	5470	1.46
25	*rac*-**13**	300	6 h	82	9700	7550	1.58
26	*rac*-**13**	300	24 h	92	10500	8910	1.65
27	*rac*-**13**	600	24 h	87	13700	10900	1.55
28	*rac*-**14**	300	2 h	8	-	-	-
29	*rac*-**14**	300	6 h	60	7830	5200	1.22
30	*rac*-**14**	300	24 h	90	11000	12000	1.42

Table 1. Polymerisation data for **10**-**14** in the ROP of *rac*-lactide under solution and melt polymerisation conditions. [a] Conversion from ^{1}H NMR spectra evaluated by integration of the methine regions of polylactide versus lactide. [b] Polymer number average molar mass determined from GPC traces. [c] Calculated polymer molecular weight by ^{1}H NMR end-group analysis. [d] Polydispersity indices (M_w / M_n) obtained from GPC traces.

bridging carboxylate. The initiating site ***A*** is proposed to be too far away from the chiral centre on the pendant arm to be influenced by it. In contrast, the ***A**** sit is in close proximity and therefore able to impart a degree of stereoselective control over the polymerisation.

Under solution polymerisation conditions, there is a disparity in the activity between the achiral/chiral analogues **11**/*rac*-**13** and **12**/*rac*-**14**. Lower conversion from monomer to polymer was observed. Although the *X* group was seen to reduce aggregation in *rac*-**13** and *rac*-**14**, we envisage the *X* group causes greater steric hindrance for both monomer and polymer chain approach to the titanium centre, in turn reducing the activity of the compounds. In contrast, **11**/*rac*-**13** and **12**/*rac*-**14** show very similar performance in the ROP of *rac*-lactide under melt polymerisation conditions, with good agreement between the conversion, M_n and PDI values.

The microstructure of the polylactide produced by **10**-**14** was inspected using ^{1}H{^{1}H} NMR spectroscopy. The P_m values indicate a slightly heterotactic polymer was obtained using initiators **10**-**12**.[40-43] Calculating the M_n from the ^{1}H NMR of the polylactide chain agree for the most part with the M_n values obtained from GPC, suggesting linear polylactide is produced. Isotactic enrichment was inspected by comparing the effectiveness of site control mechanism (SCM)[41] or chain end control mechanism (CEM)[42] statistics for tetrad intensity prediction followed by comparison of the P_m value between the achiral and chiral initiators (Table S2). The SCM statistical model failed to predict the tetrad intensities for polylactide samples produced by *rac*-**13**, in which case CEM statistics were more appropriate. For polylactide samples produced by *rac*-**14**, SCM statistics were more successful in the prediction of tetrad intensities than CEM statistics. Thus, for *rac*-**14** we see an increase in intensity of the mmm tetrad (and P_m) associated with an increase in influence of a SCM over enchainment during the polymerisation. The lack of stereoselectivity imparted by *rac*-**13** in comparison to *rac*-**14** can be explained by referring to Figure 3. The achiral site ***A*** is not sterically disfavoured in *rac*-**13** due to the lack of *tert*-butyl groups in the *R''* positions. With no differentiation between the achiral and chiral sites, the influence on stereoselectivity imparted by *rac*-**13** was minimal. A semi logarithmic plot of lactide consumption against time gives a linear fit for both *rac*- and *L*-lactide, from which the

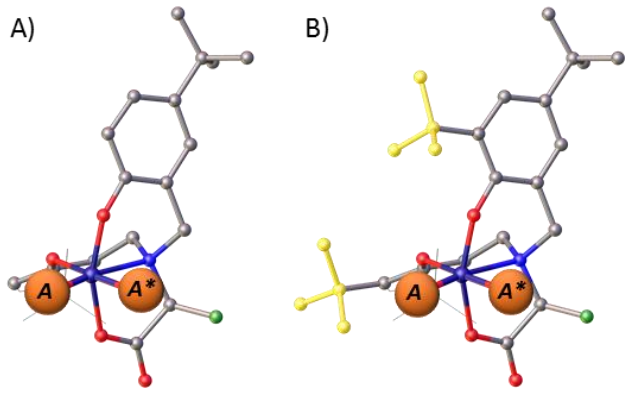

Figure 3. Models showing the achiral (***A***) and chiral (***A****) sites for: A) *S*-**13** B) *S*-**14**; constructed using a mononuclear unit from the asymmetric unit of $\mathbf{12}_3$(HO*i*Pr). A portion of the model is displayed as wireframe for clarity. Yellow: *tert*-butyl groups in the *R''* positions. Green: methyl group in the *X* position. Orange: achiral (***A***) and chiral (***A****) sites. Purple: titanium. Grey: carbon. Blue: nitrogen. Red: oxygen.

observed rate constant k_{app} was calculated to be 2.89×10^{-2} min^{-1} and 2.44×10^{-2} min^{-1} respectively. The almost equal rates indicate there is no preference for *rac*- or *L*-lactide consumption by *rac*-**14**. However, we remain cautious over our assignment of mechanism as the challenges in distinguishing between SCM and CEM are well documented.[43-46]

Conclusions

To study the effect of aggregation of the initiator in the ROP of *rac*-lactide we undertook an in-depth study to define a trend between nuclearity and activity, We successfully synthesised and characterised a series of polynuclear titanium complexes stabilised by a multidentate amine bis(phenolate) ligand featuring a bridging carboxylate donor. These compounds presented themselves as dynamic mixtures of different nuclearities. An in-depth solution-state NMR study was key to develop our understanding of the aggregates in solution and relate their behaviour to their performance in the ROP of *rac*-lactide. Subsequently, ^{1}H DOSY NMR studies probed the size distributions of aggregates in solution, establishing a trend: increasing steric bulk around the ligand periphery reduced the nuclearity of the aggregates. These aggregates were applied to the ROP of *rac*-lactide under solution and melt polymerisation conditions. Increasing the steric bulk of the peripheral phenolate groups resulted in an increase in activity. The largest, with di-*tert*-butyl phenolate donors, was observed to significantly increase the activity of the polynuclear complex, which we attribute to restricted aggregation of the titanium species. Unfortunately, this group also hindered polymerisation under melt conditions due to the restriction it causes about the titanium centre – a contrasting result to our previous findings whereby enhanced solubility had the greatest influence over activity under melt polymerisation conditions.[19] Finally, a chiral backbone was introduced to the ligand framework to form analogous titanium species with both achiral and chiral sites. When steric bulk hindered access to the achiral site, a SCM imparted a greater degree of isotactic enchainment in the polylactide chain. These polynuclear titanium aggregates showcase how careful design on the molecular scale can have a great effect on the performance of initiators and macromolecular properties of the polymer they produce. Using this new understanding, our focus will be to increase the activity of new polynuclear initiators and the isotactic enchainment they can impart to the polymer under industrially-viable conditions.

Experimental

The starting materials were purchased and used as received from Sigma-Aldrich and Acros except for *rac*- and *L*-lactide, which were sublimed and stored under a dry N_2 atmosphere prior to use. Dry solvents were purified in an MBRAUN SPS-800 and stored over 4 Å molecular sieves under a dry N_2 atmosphere. NMR spectroscopy data was acquired with a Bruker AVIII 300 MHz instrument or Bruker AVIII 400 MHz at 298 K unless otherwise stated. ^{1}H DOSY NMR experiments were recorded on a Bruker AVIII 400 MHz with samples at 50 nM concentration and tetramethylsilane standard. Electrospray ionisation (ESI) and electron impact ionisation (EI) were recorded using a Bruker micrOTOF II. Nanoelectrospray ionisation (NSI) and matrix-assisted laser desorption (MALDI) mass spectra were obtained by the EPSRC National Mass Spectrometry Facility (NMSF), Swansea, UK. Elemental microanalysis was carried out on an Exeter CE-440 Elemental Analyse. Single crystal X-ray diffraction data was acquired using a Bruker Apex-II operating at 173 K with Mo-K_α radiation or Rigaku SuperNova operating at 120 K with Cu-K_α radiation. CCDC 1562058 and 1562059 contain the supplementary crystallographic data for this paper. These data can be obtained free of charge from The Cambridge Crystallographic Data Centre. Molecular weights (M_n) and molecular mass distributions (M_w / M_n) of polymers were determined by GPC at 35°C using THF as eluent with a flow rate of 1.0 mL min^{-1}. The experimental values were obtained relative to a calibration curve using polystyrene standards, which were corrected with Mark-Houwink parameters and by a factor of 0.58.[47]

Synthesis of ligand precursors

4$(H)_3$[48,49]:

Sodium hydroxide (0.80 g, 20 mmol) was dissolved in methanol (30 mL) with 2,4-di-*tert*-butylphenol (8.253 g, 40 mmol) and glycine (1.50 g, 20 mmol). Paraformaldehyde (1.20 g, 40 mmol) was added and the reaction mixture was heated to reflux for 48 h under N_2. A white precipitate formed and was filtered, washed with 3×30 mL ice-cold methanol and dried. Yield: 6.834 g (66.8 %). ^{1}H NMR (300 MHz, $CDCl_3$): δ 7.22 (d, 2H, ArH), 6.89 (d, 2H, ArH), 3.69 (s, 4H, CH_2), 3.29 (s, 2H, CH_2), 1.40 (s, 18H, CH_3), 1.29 (s, 18H, CH_3); ^{13}C NMR (75.5 MHz, $CDCl_3$): δ 171.4, 152.7, 141.2, 136.3, 125.2, 124.2, 120.0, 60.5, 57.3, 34.9, 34.1, 31.6, 29.6; HRMS (ESI$^+$): m/z calcd for $C_{32}H_{50}NO_4$: 512.3734 $[M+H]^+$; found 512.3709; elemental analysis calcd (%) for $C_{32}H_{49}NO_4$: C, 75.11; H, 9.65; N, 2.74; found: C 74.98; H 9.52; N 2.69.

rac-**5**$(H)_3$:

Sodium hydroxide (0.80 g, 20 mmol) was dissolved in methanol (30 mL) with 4-*tert*-butylphenol (4.326 g, 40 mmol) and *S*-alanine (1.782 g, 20 mmol). Paraformaldehyde (1.20 g, 40 mmol) was added and the reaction mixture was heated to reflux for 72 h under N_2. The solvents were removed to give off-white solids that were dissolved in methanol (30 mL). The yellow solution was acidified with aqueous 1 M hydrochloric acid and the white precipitate collected and dried. The product was isolated by column chromatography (gradient 90:10 to 50:50, dichloromethane : ethyl acetate with 0.1 % acetic acid) as a white powder. Yield: 4.036 g (48.8 %). ^{1}H NMR (400 MHz, $CDCl_3$): δ 7.17 (d, 2H, ArH), 7.03 (s, 2H, ArH), 6.87 (d, 2H, ArH), 4.53 (br, 2H, CH_2), 4.18 (br, 2H, CH_2). 3.86 (br, 1H, CH), 1.58 (br, 3H, CH_3), 1.18 (s, 18H, CH_3); ^{13}C NMR (100.6 MHz, $CDCl_3$): δ 176.2, 154.3, 142.2, 128.0, 127.7, 116.7, 116.1, 60.6, 59.9, 53.8, 31.5, 14.2; HRMS (ESI$^+$): m/z calcd for $C_{25}H_{36}NO_4$: 414.2642 $[M+H]^+$; found 414.2657; elemental analysis calcd (%) for $C_{25}H_{35}NO_4$: C, 72.61; H, 8.53; N, 3.39; found: C 72.32; H 8.22; N 3.31.

rac-**6**$(H)_3$:

Sodium hydroxide (0.80 g, 20 mmol) was dissolved in methanol (30 mL) with 2,4-di-*tert*-butylphenol (8.253 g, 40 mmol) and glycine (1.50 g, 20 mmol). Paraformaldehyde (1.20 g, 40 mmol) was added and the reaction mixture was heated to reflux for 96 h under N_2. The solvents were removed to give off-white solids that were dissolved in methanol (30 mL). The yellow solution was acidified with aqueous 1 M hydrochloric acid and the white precipitate collected and dried. The product was isolated by column chromatography (gradient 95:5 to 70:30, dichloromethane : ethyl acetate with 0.1 % acetic acid) as a white powder. Yield: 6.224 g (59.2 %). 1H NMR (300 MHz, CDCl3): δ 7.16 (d, 2H, ArH), 6.81 (d, 2H, ArH), 4.11 (d, 2H, CH2), 3.73 (q, 1H, CH), 3.36 (d, 2H, CH2), 1.38 (d, 3H, CH3), 1.30 (s, 18H, CH3), 1.19 (s, 18H, CH3); 13C NMR (75.5 MHz, CDCl3): δ 174.5, 152.8, 141.2, 136.3, 125.2, 124.1, 119.9, 60.3, 55.9, 53.0, 34.9, 34.1, 31.6, 29.6, 14.3; HRMS (ESI+): m/z calcd for C33H52NO4: 526.3890 [M+H]+; found 526.3883 ; elemental analysis calcd (%) for $C_{33}H_{51}NO_4$: C, 75.39; H, 9.78; N, 2.66; found: C 75.30; H 9.54; N 2.67.

Synthesis of titanium complexes

The dynamic nature of these polynuclear titanium aggregates leads to complex NMR spectra. For **10**-**14**, NMR data will be presented for the complex in $CDCl_3$ followed by $CDCl_3$ with DMAP inserted as a strong donor to reduce aggregation. Additional data for **12** in CD_6SO was also obtained and displayed two sets of signals with a 1:0.4 ratio.

General method

Under N_2, Ti(O*i*Pr)$_4$ (0.154 mL, 0.500 mmol) was added to a suspension of the ligand precursor (0.500 mmol) in dry THF (5 mL). The yellow/orange reaction mixture was stirred for 2 h after which solvents were removed under vacuum.

Complex **9**

The yellow solid was suspended in dry toluene, filtered, dried and weighed. Yield: 0.3764 g (96.2 %). ^{1}H NMR (400 MHz, 293 K, inferred by HMQC): δ 9.67-5.49 (ArH), 6.70-5.92 (CH), 5.25-4.01 (CH_2), 3.66-2.21 (CH_3); ^{13}C CP-MAS NMR (100.6 MHz, 293 K): δ 182.2, 181.7, 181.5, 165.6, 161.9, 160.3, 133.5, 131.3, 130.4, 129.6, 129.0, 127.8, 127.2, 125.6, 125.3, 124.6, 124.0, 122.9, 121.5, 120.0, 118.3, 115.9, 115.0, 114.5, 82.6, 81.0, 64.7, 63.7, 63.2, 62.9, 60.9, 59.9, 27.0, 26.1, 24.8; MS (EI): m/z calcd for $C_{19}H_{21}NO_5Ti$: 391.2 $[M]^{\cdot+}$; found 391.1; elemental analysis calcd (%) for $C_{19}H_{21}NO_5Ti$: C, 58.33; H, 5.41; N, 3.58; found: C 59.76; H 5.48; N 3.49.

Complex **10**

The yellow solid was suspended in dry acetonitrile, filtered, dried and weighed. Yield: 0.3668 (87.5 %). ^{1}H NMR (400 MHz, $CDCl_3$): δ 7.14-5.99 (m, 6H, ArH), 5.27-2.50 (m, 7H, CH / CH_2), 2.41-0.74 (m, 15H, CH_3); ^{1}H NMR (400 MHz, $CDCl_3$ / DMAP): δ 8.23 (br, 2H, ArH DMAP), 7.03-6.24 (br, 8H, ArH / ArH DMAP), 4.66 (br, 1 H, CH), 3.96 (m, 0.5H, CH), 3.68 (br, 2H, CH_2), 3.24 (br, 2H, CH_2), 2.96 (s, 6H, CH_3 DMAP), 2,18 (br, 6H, CH_3), 1.17 (br, 10H, CH_3); ^{13}C NMR (100.6 MHz, $CDCl_3$ / DMAP): δ 181.8, 174.6 (br), 164.0, 158.7, 155.1, 149.2 (br), 130.3 (br), 130.1, 130.0, 129.8, 129.7, 129.0 (br), 128.8, 125.7, 125.0, 123.9, 116.7, 115.9, 115.8, 106.6, 81.1 (br), 64.6, 64.4, 62.5, 60.0, 39.1, 25.4, 24.5, 20.6, 20.5; MS (MALDI): m/z calcd for $C_{24}H_{34}NO_6Ti$: 480.2 $[M+H+HOiPr]^+$; found 480.1. HRMS (ESI$^-$): m/z calcd for $C_{21}H_{28}NO_5Ti$: 422.1447 $[M+(H)_3]^-$; found 422.1146; elemental analysis calcd (%) for $C_{21}H_{25}NO_5Ti$: C, 60.15; H, 6.01; N, 3.34; found: C 61.99; H 6.74; N 3.28.

Complex **11**

The orange solid was suspended in dry acetonitrile, filtered, dried and weighed. Yield: 0.4286 (85.1 %). ^{1}H NMR (400 MHz, $CDCl_3$): δ 7.26-6.21 (m, 6H, ArH), 5.42-2.61 (m, 7H, CH / CH_2), 2.11-0.79 (m, 24H, CH_3); ^{1}H NMR (400 MHz, $CDCl_3$ / DMAP): δ 8.22 (br, 2H, ArH DMAP), 7.17 (d, 2H, ArH), 6.96 (s, 2H, ArH), 6.71 (br, 2H, ArH), 6.41 (d, 2H, ArH DMAP), 4.67 (br, 1H, CH), 3.96 (m, 0.5H, CH), 3.77 (br, 2H, CH_2), 3.24 (br, 2H, CH_2), 2.96 (s, 6H, CH_3 DMAP), 1.17 (br, 28H, CH_3); ^{13}C NMR (100.6 MHz, $CDCl_3$ / DMAP): δ 181.7, 174.7 (br), 163.5, 158.5, 154.8 (br), 149.3 (br), 142.5 (br), 126.5 (br), 126.0, 124.7, 123.5 (br), 116.4 (br), 106.6, 80.8 (br), 64.4, 63.4 (br), 39.2, 34.1, 31.6, 25.4, 24.6; HRMS (ESI$^-$): m/z calcd for $C_{27}H_{40}NO_5Ti$: 506.2386 $[M+(H)_3]^-$; found 506.2104; elemental analysis calcd (%) for $C_{27}H_{37}NO_5Ti$: C, 64.41; H, 7.41; N, 2.78; found: C 65.37; H 7.35; N 2.62.

Complex **12**

The orange solid was dissolved in dry THF. Clear, orange crystals were obtained at –20 °C which were filtered, dried and weighed. Yield: 0.5236 g (85.0 %). ^{1}H NMR (400 MHz, $CDCl_3$): δ 10.41 (d, 0.1H, C=O···HO*i*Pr), 7.38-6.55 (m, 4H, ArH), 5.45-2.34 (m, 7H, CH / CH_2), 1.83-0.67 (m, 42H, CH_3); ^{1}H NMR (400 MHz, $CDCl_3$ / DMAP): δ 8.46 (d, 0.75H, ArH DMAP), 8.20 (br, 3.25H, ArH DMAP), 7.19 (d, 2H, ArH), 6.83 (d, 2H, ArH), 6.41 (m, 4H, DMAP), 4.46 (sept, 0.75H, CH), 3.95 (sept, 1H, CH), 3.78 (d, 1H, CH_2), 3.35 (s, 1H, CH_2), 3.22 (br, 1H, CH_2), 3.15 (d, 1H, CH_2), 2.96 (m, 12H, DMAP), 1.45 (m, 18H, CH_3), 1.21 (m, 18H, CH_3), 1.13 (d, 6H, CH_3), 1.08 (d, 2.5H, CH_3), 1.00 (d, 2.5H, CH_3); ^{1}H NMR (400 MHz, CD_6SO): δ 7.12 (br, 2H, ArH), 7.06 (m, 0.4H, ArH), 7.00 (m, 2H, ArH), 6.87 (m. 0.4H, ArH), 5.01 (br, 0.8H, CH), 4.28 (m, 0.4H, CH_2), 4.04 (s, 1.5H, CH_2), 3.78 (sept, 2H, CH), 3.48 (m, 3H, CH_2), 3.25 (m, 0.4H, CH_2), 2.88 (d, 0.4H, CH_2), 2.78 (br, 1,5H, CH_2), 1.41 (m, 25.2H, CH_3), 1.23 (m, 25.2H, CH_3), 1.05 (m, 16.2H, CH_3); ^{13}C NMR (100.6 MHz, $CDCl_3$ / DMAP): δ 175.0, 174.0, 160.1, 155.3,

154.7, 150.4, 149.4, 141.5, 141.3, 136.1, 135.3 (br), 125.0, 124.3, 124.2, 124.0, 123.6, 106.6, 106.3, 80.9, 79.7, 64.3, 64.2, 63.8, 62.5 (br), 57.6, 39.2, 39.1, 35.2, 35.1, 34.3, 31.7, 29.9, 29.8, 25.4, 25.3; MS (MALDI): m/z calcd for $C_{35}H_{53}NO_5Ti$: 615.3 $[M+H]^+$; found 615.3; elemental analysis calcd (%) for $C_{35}H_{53}NO_5Ti$: C, 68.28; H, 8.68; N, 2.28; found: C 69.78; H 9.00; N 2.20.

Complex *rac*-**13**

The orange solid was dissolved in dry toluene. An orange precipitate was obtained at –20 °C which was filtered, washed, dried and weighed. Yield: 0.4857 g (93.9 %). ^{1}H NMR (400 MHz, $CDCl_3$): δ 7.19 (d, 1H, ArH), 7.15 (dd, 1H, ArH), 7.02 (d, 1H, ArH), 6.97 (d, 1H, ArH), 6.54 (t, 2H, ArH), 4.67 (sept, 1H, CH), 4.28 (d, 1H, CH_2), 4.07 (sept, 1H, CH), 3.53 (d, 1H, CH_2), 3.43 (d, 1H, CH_2), 3.23 (q, 1H, CH), 3.07 (d, 1H, CH_2), 1.45 (d, 3H, CH_3), 1.32 (m, 30H, CH_3); ^{1}H NMR (400 MHz, $CDCl_3$ / DMAP): δ 8.19 (br, 2H, ArH DMAP), 7.17 (dd, 1H, ArH), 7.12 (br, 1H, ArH), 7.00 (d, 1H, ArH), 6.97 (br, 1H, ArH), 6.77 (d, 1H, ArH), 6.59 (d, 1H, ArH), 6.40 (d, 2H, ArH DMAP), 4.73 (br, 1H, CH), 3.95 (sept, 1H, CH), 3.63 (d, 1H, CH_2), 3.48 (m, 3H, CH_2 / CH), 3.10 (m, 1H, CH_2), 2.94 (s, 6H, CH_3 DMAP), 1.22 (s, 9H, CH_3), 1.18 (m, 12H, CH_3), 1.13 (d, 12H, CH_3); ^{13}C NMR (100.6 MHz, $CDCl_3$ / DMAP): δ 176.4, 164.2 (br), 159.6 (br), 154.7 (br), 149.6 (br), 142.7, 141.7, 126.4, 124.1, 123.1, 116.6, 115.5, 106.6, 80.7 (br), 77.3, 77.0, 76.7, 64.3 (br), 61.1, 39.0, 34.1, 34.0, 31.6, 31.6, 25.4, 24.6, 24.5, 9.1; MS (EI): m/z calcd for $C_{31}H_{47}NO_6Ti$: 577.3 $[M+HO{\it i}Pr]^{\cdot+}$; found 577.5; m/z calcd for $C_{28}H_{40}NO_5Ti$: 518.2 $[M+H]^{\cdot+}$; found 518.2; elemental analysis calcd (%) for $C_{28}H_{39}NO_5Ti$: C, 64.99; H, 7.60; N, 2.71; found: C 66.53; H 7.87; N 2.79.

Complex *rac*-**14**

The orange solid was dissolved in dry THF. An orange precipitate was obtained at –20 °C which was filtered, washed, dried and weighed. Yield: 0.5692 g (90.4 %). ^{1}H NMR (400 MHz, $CDCl_3$): δ 7.21 (dd, 2H, ArH), 6.96 (d, 1H, ArH), 6.84 (d, 1H, ArH), 4.49 (sept, 1H, CH), 4.03 (m, 3.5H, CH_2), 3.82 (q, 1H, CH), 3.40 (d, 0.75H, CH_2), 3.32 (d, 0.75H, CH_2), 1.56 (d, 3H, CH_3), 1.49 (d, 9H, CH_3), 1.44 (d, 9H, CH_3), 1.29 (d, 9H, CH_3), 1.26 (d, 15H, CH_3); ^{1}H NMR (400 MHz, $CDCl_3$ / DMAP): δ 8.26 (br, 2H, ArH DMAP), 7.21 (d, 1H, ArH), 7.10 (br, 1H, ArH), 6.87 (m, 2H, ArH), 6.38 (d, 2H, ArH DMAP), 4.46 (br, 1H, CH), 3.94 (sept, 0.5H, CH), 3.56 (m, 2H, CH_2 / CH), 3.36 (d, 1H, CH_2), 3.00 (d, 2H, CH_2), 2.95 (s, 6H, CH_3 DMAP), 1.48 (s, 9H, CH_3), 1.37 (m, 12H, CH_3), 1.22 (s, 9H, CH_3), 1.16 (s, 9H, CH_3), 1.12 (d, 3H, CH_3), 1.03 (d, 3H, CH_3), 0.95 (d, 3H, CH_3); ^{13}C NMR (100.6 MHz, $CDCl_3$ / DMAP): δ 176.7, 163.1 (br), 158.8, 155.0, 149.5 (br), 141.4, 140.8, 136.3, 135.1, 124.7, 124.5 (br), 124.3 (br), 124.1, 123.6, 123.3, 106.6, 79.6 (br), 65.1 (br), 64.3, 61.4, 53.0 (br), 39.1, 35.2, 34.8, 34.3, 34.2, 31.7, 31.7, 29.9, 29.9, 25.4, 25.3, 9.4; MS (EI): m/z calcd for $C_{36}H_{56}NO_5Ti$: 630.4 $[M+H]^{\cdot+}$; found 630.3; elemental analysis calcd (%) for $C_{36}H_{55}NO_5Ti$: C, 68.67; H, 8.80; N, 2.22; found: C 69.94; H 8.61; N 2.19.

Solution polymerisation procedure

Under N_2, a Schlenk flask was charged with *rac*-lactide (1.00 g, 6.94 mmol) and an appropriate amount of catalyst. Dry toluene (6.94 mL) was added and the vessel was heated in an oil bath at 130 °C. Once the polymerisation time was reached, the vessel was removed from the oil bath and the reaction terminated by the addition of methanol (5 mL). The solvents were removed and the resulting solids were dissolved in dichloromethane. The polymers were precipitated with excess methanol, washed with methanol and dried at 40 °C under vacuum.

Melt polymerisation procedure

Under N_2, a vessel was charged with sublimed *rac*-lactide (1.00 g, 6.94 mmol) and appropriate amounts of catalyst. The vessel was sealed and immersed in an oil bath at 130°C. Once polymerisation time was reached, the vessel was removed from the oil bath and the reaction terminated by the addition of the methanol (5 mL). The solids were dissolved in dichloromethane and the polymers were dissolved with excess methanol. The collected polymers were washed with methanol and dried at 40°C under vacuum.

Conflicts of interest

There are no conflicts to declare.

Acknowledgements

We are grateful to acknowledge financial support from Heriot-Watt University and assistance from the EPSRC UK National Mass Spectrometry Facility at Swansea University, UK. This research used resources of the Advanced Light Source, which is a DOE Office of Science User Facility under contract no. DE-AC02-05CH11231.

References

1 P. J. Dijkstra, H. Z. Du and J. Feijen, *Polym Chem-Uk*, 2011, **2**, 520-527.
2 M. Shavit and E. Y. Tshuva, *Eur. J. Inorg. Chem.*, 2008, 1467-1474; J.D. Ryan, K.J. Gagnon, S.J. Teat and R.D. McIntosh, *Chem. Commun*., 2016, **52**, 9071-9073
3 B. T. Ko and C. C. Lin, *J. Am. Chem. Soc.*, 2001, **123**, 7973-7977.
4 Z. H. Liang, M. Zhang, X. F. Ni, X. Li and Z. Q. Shen, *Inorg. Chem. Commun.*, 2013, **29**, 145-147.
5 D. C. Aluthge, E. X. Yan, J. M. Ahn and P. Mehrkhodavandi, *Inorg. Chem.*, 2014, **53**, 6828-6836.
6 K. M. Osten, D. C. Aluthge and P. Mehrkhodavandi, *Dalton Trans.*, 2015, **44**, 6126-6139.
7 F. M. Garcia-Valle, R. Estivill, C. Gallegos, T. Cuenca, M. E. G. Mosquera, V. Tabernero and J. Cano, *Organometallics*, 2015, **34**, 477-487.
8 D. C. Aluthge, J. M. Ahn and P. Mehrkhodavandi, *Chem Sci*, 2015, **6**, 5284-5292.
9 A. Thevenon, C. Romain, M. S. Bennington, A. J. P. White, H. J. Davidson, S. Brooker and C. K. Williams, *Angewandte Chemie-International Edition*, 2016, **55**, 8680-8685; Y. J. Kim and J. G. Verkade, *Macromol. Rapid Commun.*, 2002, **23**, 917-921.
10 For select examples of organometallic aggregates see: A.Arbaoui, C. Redshaw and D.L. Hughes, *Chem. Commun*. 2008, **39**, 4717−4719; M. Normand, T. Roisnel, J.F. Carpentier and E. Kirillov, *Chem. Commun*. 2013, **49**, 11692−11694; S.M. Kirk, H.C. Quilter, A. Buchard, L.H. Thomas, G. Kociok-Kohn and M.D. Jones, *Dalton Trans*. 2016, **45**, 13846−13852; F.

Isnard, M. Lamberti. L. Lettieri, I. D'Auria, K. Press, R. Troiano and M. Mazzeo, *Dalton Trans.* 2016, **45**, 16001-16010; Y. Gao, Z. Dai, J. Zhang, X. Ma, N. Tang and J. Wu, *Inorg. Chem*. 2014, **53**, 716-726; X.Pang , R.Duan, X.Li, C. Hu, X. Wang and X. Chen, *Macromolecules*, 2018, **51**, 906-913.
11 P. Dubois, C. Jacobs, R. Jerome and P. Teyssie, *Macromolecules*, 1991, **24**, 2266-2270.
12 A. Kowalski, A. Duda and S. Penczek, *Macromolecules*, 1998, **31**, 2114-2122.
13 W. M. Stevels, M. J. K. Ankone, P. J. Dijkstra and J. Feijen, *Macromolecules*, 1996, **29**, 6132-6138.
14 B. J. O'Keefe, S. M. Monnier, M. A. Hillmyer and W. B. Tolman, *J. Am. Chem. Soc.*, 2001, **123**, 339-340.
15 B. J. O'Keefe, L. E. Breyfogle, M. A. Hillmyer and W. B. Tolman, *J. Am. Chem. Soc.*, 2002, **124**, 4384-4393.
16 For other example of catalysts incorporating amino acids see: D.J. Darensbourg and O. Karroonnirun, Inorg. Chem., 2010, 49, 2360-2371; Organometallics 2010, 29, 5627-5634; D.J. Darensbourg, O. Karroonnirun and S.J. Wilson, Inorg. Chem., 2011, 50, 6775-6787; R. L. Webster, RSC Adv., 2014, 4, 5254-5260; Y. F. Al-Khafaji, T.J. Prior, L. Horsburgh, M.R.J. Elsegood, C. Redshaw, ChemistrySelect, 2017, 2, 759-768; Y. F. Al-Khafaji, M.R.J. Elsegood, J.W.A. Frese, C. Redshaw, RSC Adv., 2017, 7, 4510-4517.
17 A. S. Ceccato, A. Neves, M. A. De Brito, S. M. Drechsel, A. S. Mangrich, R. Werner, W. Haase and A. J. Bortoluzzi, *J. Chem. Soc., Dalton Trans.*, 2000, 1573-1577; Y.-L. Wong, Y. Yan, E. S. H. Chan, Q. Yang, T. C. W. Mak and D. K. P. Ng, *J. Chem. Soc., Dalton Trans.*, 1998, 3057-3064.
18 Z. Taheri, B. Ghanbari and H. Hajibabaei, *Chem. Pap.*, 2014, **68**, 989-994.
19 J. M. E. P. Cols, C. E. Taylor, K. J. Gagnon, S. J. Teat and R. D. McIntosh, *Dalton Trans.*, 2016, **45**, 17729-17738.
20 S. Barroso, P. Adao, A. M. Coelho, J. C. Pessoa and A. M. Martins, *J. Mol. Catal. A: Chem.*, 2016, **412**, 107-116.
21 G. G. Smith and T. Sivakua, *J. Org. Chem.*, 1983, **48**, 627-634.
22 E. D. Stroud, D. J. Fife and G. G. Smith, *J. Org. Chem.*, 1983, **48**, 5368-5369.
23 R. Baum and G. G. Smith, *J. Am. Chem. Soc.*, 1986, **108**, 7325-7327.
24 24. A. J. Chmura, M. G. Davidson, M. D. Jones, M. D. Lunn, M. F. Mahon, A. F. Johnson, P. Khunkamchoo, S. L. Roberts and S. S. F. Wong, *Macromolecules*, 2006, **39**, 7250-7257.
25 25. E. Y. Tshuva, M. Versano, I. Goldberg, M. Kol, H. Weitman and Z. Goldschmidt, *Inorg. Chem. Commun.*, 1999, **2**, 371-373.
26 E. Y. Tshuva, I. Goldberg, M. Kol and Z. Goldschmidt, *Inorg. Chem.*, 2001, **40**, 4263-4270.
27 G. A. Jeffrey, *Crystallography Reviews*, 2003, **9**, 135-176.
28 D. T. Dugah, B. W. Skelton and E. E. Delbridge, *Dalton Trans.*, 2009, 1436-1445.
29 S. Barroso, A. M. Coelho, S. Gomez-Ruiz, M. J. Calhorda, Z. Zizak, G. N. Kaluderovic and A. M. Martins, *Dalton Trans.*, 2014, **43**, 17422-17433.
30 R. Neufeld and D. Stalke, *Chem Sci*, 2015, **6**, 3354-3364.
31 S. Bachmann, R. Neufeld, M. Dzemski and D. Stalke, *Chem-Eur J*, 2016, **22**, 8462-8465.
32 B. Gupta, N. Revagade and J. Hilborn, *Prog. Polym. Sci.*, 2007, **32**, 455-482.
33 C. K. Williams, *Chem. Soc. Rev.*, 2007, **36**, 1573-1580.
34 S. Slomkowski, S. Penczek and A. Duda, *Polym. Adv. Technol.*, 2014, **25**, 436-447.
35 T. Rosen, I. Goldberg, W. Navarra, V. Venditto and M. Kol, *Chem Sci*, 2017.
36 D. Takeuchi, T. Nakamura and T. Aida, *Macromolecules*, 2000, **33**, 725-729.
37 A. Sauer, A. Kapelski, C. Fliedel, S. Dagorne, M. Kol and J. Okuda, *Dalton Trans.*, 2013, **42**, 9007-9023.
38 Y. Ikada, K. Jamshidi, H. Tsuji and S. H. Hyon, *Macromolecules*, 1987, **20**, 904-906.
39 M. J. Stanford and A. P. Dove, *Chem. Soc. Rev.*, 2010, **39**, 486-494.
40 M. Bouyahyi, N. Ajellal, E. Kirillov, C. M. Thomas and J. F. Carpentier, *Chem-Eur J*, 2011, **17**, 1872-1883. For an alternative method of assigning P_r see: M.J. Walton, S.J. Lancaster, C. Redshaw, *ChemCatChem*, 2014, **6**, 1892-1898.
41 T. M. Ovitt and G. W. Coates, *J. Am. Chem. Soc.*, 2002, **124**, 1316-1326.
42 B. M. Chamberlain, M. Cheng, D. R. Moore, T. M. Ovitt, E. B. Lobkovsky and G. W. Coates, *J. Am. Chem. Soc.*, 2001, **123**, 3229-3238.
43 Y. Q. Cui, C. J. Chen, Y. Y. Sun, J. C. Wu and X. B. Pan, *Inorg Chem Front*, 2017, **4**, 261-269.
44 Z. H. Tang, X. S. Chen, Y. K. Yang, X. Pang, J. R. Sun, X. F. Zhang and X. B. Jing, *J Polym Sci Pol Chem*, 2004, **42**, 5974-5982.
45 H. B. Wang, Y. Yang and H. Y. Ma, *Macromolecules*, 2014, **47**, 7750-7764.
46 A. Pilone, N. De Maio, K. Press, V. Venditto, D. Pappalardo, M. Mazzeo, C. Pellecchia, M. Kol and M. Lamberti, *Dalton Trans.*, 2015, **44**, 2157-2165.
47 T. Biela, A. Duda and S. Penczek, *Macromol. Symp.*, 2002, **183**, 1-10.
48 E. Safaei, H. Sheykhi, A. Wojtczak, Z. Jaglicic and A. Kozakiewicz, *Polyhedron*, 2011, **30**, 1219-1224.
49 T. Weyhermuller, R. Wagner and P. Chaudhuri, *Eur. J. Inorg. Chem.*, 2011, 2547-2557.